doi:10.3772/j.issn.1006-6748.2020.01.007

Model-free adaptive control of space manipulator under different gravity environment①

Wen Yintang (温银堂), Gao Linqi, Liu Fucai②, Qin Li
(School of Electrical Engineering, Yanshan University, Qin Huangdao 066004, P. R. China)

Abstract

Due to the release of gravity in the space environment, the dynamic characteristics of the space manipulator have changed compared with that of the ground, which results in the change of its tracking precision. This paper presents a model-free adaptive control (MFAC) strategy to track the desired trajectory under different gravity environment. A dynamic transformation method and full form dynamic linearization (FFDL) approach are selected to dynamicly linearize the system, which can better eliminate the complex dynamics that may exist in the original system. The controlled object uses the two degrees of freedom of space manipulator and the controller only depends on the desired angle and torque of each joint of the space manipulator. Moreover, the proof of stability is also provided. Finally, simulation results are presented to demonstrate the effectiveness of the proposed strategy. It is shown that the proposed approach can achieve better trajectory tracking performance under different gravity environment without changing the control parameters, and the tracking precision can be significantly improved as compared with the proportional differential (PD) control results.

Key words: space manipulator, microgravity, model-free adaptive, trajectory tracking control

0 Introduction

Along with the increasing frequency of human space activities, the number of 'space debris' in space is increasing, and they are not beneficial for the normal operation of space vehicles and even seriously affect the safety of normal satellites[1]. In order to reduce the losses and protect the orbital resources, the national scientists have been working on on-orbit service technology for satellite maintenance and orbital garbage removal[2,3]. Using space manipulators instead of astronauts for space operations can not only avoid the damage to astronauts, but also reduce the costs and improve the benefits of space exploration. Therefore, it is necessary to design an adaptive controller to track the particular trajectory.

Due to the release of gravity in the space environment[4] and the uncertain external disturbance, the dynamic characteristics of space manipulator have changed compared with that of the ground. Once the space manipulator trajectory tracking controller is assembled on gravity environment, it will be inapplicable for microgravity environment due to the changes of dynamics characteristics, which result in the space manipulator cannot track the desired trajectory. This robot system is multi-input and multi-output nonlinear system, which has time-varying and strong coupling properties, the control of this mechanism turns to be complicated[5]. In order to achieve the end of the space manipulator trajectory tracking control, the researchers have done a lot of experiments on this topic. Walker and Wee[6] presented an adaptive control method for space manipulator, which can achieve global stablility in the presence of uncertainties in the inertial parameters. Kim and Lewis[7] proposed a robust neural network output feedback scheme for the motion control of robot manipulators without measuring the joint velocities. Qin et al.[8] proposed a fuzzy adaptive robust control strategy for space manipulator, in which the fuzzy algorithm was employed to approximate the nonlinear uncertainties in the model and achieved effective space manipulator trajectory tracking task. Qin et al.[9] proposed an adaptive back stepping sliding mode controller to eliminate the impact of parameter uncertainties and disturbances. However, when the manipulator

① Sponsored by the National Natural Science Foundation of China (No. 51605415) and Natural Science Foundation of Hebei Province (No. F2016203494, E2017203240).

② To whom correspondence should be addressed. E-mail: lfc@ysu.edu.cn

Received on Jan. 18, 2019

is in different gravity environment, it has to adjust the control law to track the trajectory, and also the above methods depend on the prior knowledge about the upper bound of the system, which is not applicable to the trajectory tracking task of manipulator in microgravity environment. For this reason, it is necessary to understand the changes of the dynamics and motion behaviour of the manipulator under different gravity environment, then design a proper controller that can track the desired trajectory in different gravity environment, which could overcome the influence of gravity changes of the space manipulator.

In recent years, model-free adaptive control (MFAC) algorithm is paid more attention by researchers in various fields. Gao et al.[10] proposed a CFDL based MFAC controller to the polishing robot, achieved a good control performance and adaptively decoupled the coupled outputs for MIMO system. Wang et al.[11] applied the MFAC method combined with sliding mode algorithm to the robotic exoskeleton tracking system, which could make the robotic exoskeleton tracking on its desired velocity tightly even when the dynamic parameter of the exoskeleton was time-varying irregularly and uncertainly. The data-driven MFAC strategy was proposed by Hou[12] in 1994 to solve the problem of inaccurate modelling of the controlled system. Hou[12] aimed to establish a nonparametric model of a nonlinear system and developed an adaptive control theory that did not depend on the mathematical model of the control system, but depended on the input/output (I/O) measurement data of the system. The core of the theory were three new dynamic linearization approaches and a novel concept of matrix[13,14] which will establish an equivalent dynamic linearized model of each dynamic working point of the closed-loop system. Inspired by the principle of the algorithm, the MFAC strategy is proposed to apply to the complicated space manipulator end trajectory tracking system. The algorithm can eliminate the dynamics changes caused by gravity changes, so that the space manipulator can be debugged on the ground environment and then achieve high accuracy trajectory tracking task in microgravity environment without changing the controller parameters.

The main contributions of this paper lie in three aspects: 1) The dynamic equation of space manipulator system is transformed dynamically, and the input-output relationship of the control system is obtained. 2) The MFAC controller is designed and the control system is constructed. 3) The simulation results show that MFAC strategy can achieve higher precision trajectory tracking task when the controller parameters are the same under different gravity environment.

The remainder of this paper is organized as follows. In Section 1, by analysing the dynamic equation of the robot, we get the structure of the control system. According to the principle of the MFAC algorithm, the dynamic equation is transformed to obtain the input-output relationship of the system, and then the stability of the controller is proved. Simulation results of the trajectory tracking system are presented in Section 2. Finally, Section 3 summarizes the conclusion of the research.

1 Space manipulator control system design

1.1 Control system design

In this paper, the controller is designed by MFAC theory and the controlled object is the 2 degrees of freedom of space manipulator. Fig. 1 shows the structure of the control system.

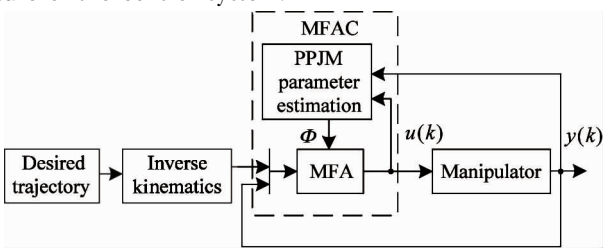

Fig. 1 MFAC control of the space manipulator system

The inputs of the space manipulator control system are the desired joint angles, which are obtained by inverse kinematics of the desired trajectory of the end. The outputs of this system are the actual joint angles of the space manipulator. By dynamic linearizing and discretizing the space manipulator dynamics system, we get the value of the state variables at each sample time. The outputs of the controller are the desired joint torques, which are also used as the input of the controller. At the same time, the differential of the desired joint angles and the differential of actual joint angles are also the inputs of the controller. By updating the value of PPJM, the joint torques of the next moment can be obtained. Through the above operations, the end trajectory tracking task of the space manipulator can be realized based on MFAC algorithm.

1.2 Transformation of the dynamics and dynamic linearization

For the space manipulator is a complex nonlinear system which cannot be directly linearized by the common approach[15], and inspired by the method proposed in Ref. [11], a method to transform and linearize the dynamical equation of the space manipulator is introduced. According to the influence of gravity, iner-

tia as well as Coriolis and centrifugal effects, its dynamics can be expressed as the following form:

$$\boldsymbol{\tau} = \boldsymbol{M}(\boldsymbol{q})\ddot{\boldsymbol{q}} + \boldsymbol{C}(\boldsymbol{q}, \dot{\boldsymbol{q}})\dot{\boldsymbol{q}} + \boldsymbol{G}(q) + \boldsymbol{f} \quad (1)$$

where $\boldsymbol{q}, \dot{\boldsymbol{q}}, \ddot{\boldsymbol{q}} \in \boldsymbol{R}^n$ represent the vector of joint position, velocity and acceleration respectively; $\boldsymbol{M}(\boldsymbol{q}) \in \boldsymbol{R}^{n\times n}$ denotes the inertia matrix, which satisfies to be positive-definite symmetric; $\boldsymbol{C}(\boldsymbol{q}, \dot{\boldsymbol{q}}) \in \boldsymbol{R}^{n\times n}$ denotes the Coriolis and centripetal force coupling matrix; $\boldsymbol{G}(\boldsymbol{q}) \in \boldsymbol{R}^n$ denotes the gravitational torques; $\boldsymbol{f}$ denotes the external input disturbance forces such as friction; $\boldsymbol{\tau} \in \boldsymbol{R}^n$ denotes a generalized driving forces.

Assuming that the input of the space manipulator dynamics is $\boldsymbol{u} = \boldsymbol{\tau}$, the output is $\boldsymbol{y} = \dot{\boldsymbol{q}}$, the Eq. (1) can be rewritten as a state space form:

$$\begin{cases} \ddot{\boldsymbol{q}} = \boldsymbol{M}(\boldsymbol{q})^{-1}\boldsymbol{u} - \boldsymbol{M}(\boldsymbol{q})^{-1}\boldsymbol{C}(\boldsymbol{q},\dot{\boldsymbol{q}})\dot{\boldsymbol{q}} \\ \qquad - \boldsymbol{M}(\boldsymbol{q})^{-1}(\boldsymbol{G}(\boldsymbol{q}) + \boldsymbol{f}) \\ \boldsymbol{y} = \dot{\boldsymbol{q}} \end{cases} \quad (2)$$

By discretization of the equation, the joint position, joint velocity and joint acceleration in Eq. (1) become specific values $\boldsymbol{q}(k)$, $\dot{\boldsymbol{q}}(k)$, $\ddot{\boldsymbol{q}}(k)$ at time k respectively. Similarly, the values of the coefficients in the equation at time k are $\boldsymbol{M}(\boldsymbol{q}(k))$, $\boldsymbol{C}(\boldsymbol{q}(k), \dot{\boldsymbol{q}}(k))$, $\boldsymbol{G}(\boldsymbol{q}(k))$ and $\boldsymbol{f}(k)$. Therefore, the input-output relationship at time k can be approximated to the following form:

$$\begin{aligned} \dot{\boldsymbol{y}}(k) = {} & \boldsymbol{M}(k)^{-1}\boldsymbol{u}(k) - \boldsymbol{M}(k)^{-1}\boldsymbol{C}(k)\boldsymbol{y}(k) \\ & - \boldsymbol{M}(k)^{-1}(\boldsymbol{G}(k) + \boldsymbol{f}(k)) \end{aligned} \quad (3)$$

When the sampling time T of the discrete system is small enough, the following equation is got:

$$\dot{\boldsymbol{y}}(k) = \frac{\boldsymbol{y}(k+1) - \boldsymbol{y}(k)}{T} \quad (4)$$

Thus, the input-output relationship between time k and time $k+1$ can be expressed as following:

$$\begin{aligned} \boldsymbol{y}(k+1) = {} & T\boldsymbol{M}(k)^{-1}\boldsymbol{u}(k) - T\boldsymbol{M}(k)^{-1}\boldsymbol{C}(k)\boldsymbol{y}(k) \\ & - T\boldsymbol{M}(k)^{-1}(\boldsymbol{G}(k) + \boldsymbol{f}(x)) + \boldsymbol{y}(k) \end{aligned} \quad (5)$$

The above equation is the discrete transformation form of space robot dynamic model. According to this equation, the partial derivatives of $\boldsymbol{y}(k+1)$ with respect to $\boldsymbol{y}(k)$ and $\boldsymbol{u}(k)$ are continuous, Eq. (5) satisfies the Lipschitz condition, therefore, there must be time-varying parameter matrix $\boldsymbol{\Phi}(k) = [\phi_1(k), \phi_2(k)]$, which enables Eq. (5) to convert into the following full form dynamic linearized data model:

$$\boldsymbol{y}(k+1) = \phi_1(k)\Delta\boldsymbol{y}(k) + \phi_2(k)\Delta\boldsymbol{u}(k) + \boldsymbol{y}(k) \quad (6)$$

where $\| \boldsymbol{\Phi}(k) \| < b$, b is a positive constant.

1.3 MFAC controller design

1.3.1 Control law

Due to the complexity of space environment, the output of space manipulator system is not only related to the input changes of adjacent time, but also related to the output changes, these factors will affect the stability of the control system. Thus, the following control input criteria function is introduced:

$$\begin{aligned} J(\boldsymbol{u}(k)) = {} & \| \boldsymbol{y}^*(k+1) - \boldsymbol{y}(k+1) \|^2 \\ & + \lambda \| \boldsymbol{u}(k) - \boldsymbol{u}(k-1) \|^2 \end{aligned} \quad (7)$$

where $\boldsymbol{y}^*(k+1)$ is the given desired joint angular velocity. Combining Eq. (6) with Eq. (7) to derive $\boldsymbol{u}(k)$ and make it equal to zero, the following expression can be obtained:

$$\begin{aligned} \Delta\boldsymbol{u}(k) = {} & (\lambda\boldsymbol{I} + \boldsymbol{\Phi}^{\mathrm{T}}(k)\boldsymbol{\Phi}(k))^{-1}\boldsymbol{\Phi}^{\mathrm{T}}(k) \\ & \times ((\boldsymbol{y}^*(k+1) - \boldsymbol{y}(k)) \\ & - \boldsymbol{\Phi}(k)\Delta\boldsymbol{y}(k)) \end{aligned} \quad (8)$$

Simplifying the matrix inversion operation in Eq. (8), the control scheme of the 2 degrees of freedom of space manipulator can be obtained as follows:

$$\begin{aligned} \boldsymbol{u}(k) = {} & \boldsymbol{u}(k-1) + \frac{\rho_1 \dot{\phi}_2(k)(\boldsymbol{y}^*(k+1) - \boldsymbol{y}(k))}{\lambda + |\dot{\phi}_2(k)|^2} \\ & - \frac{\dot{\phi}_2(k)\rho_2 \dot{\phi}_1(k)\Delta\boldsymbol{y}(k)}{\lambda + |\dot{\phi}_2(k)|^2} \end{aligned} \quad (9)$$

where $\lambda > 0$, $\mu > 0$, $\eta \in (0, 2]$, $\rho_i \in (0, 1]$, $\varepsilon > 0$, $\hat{\boldsymbol{\Phi}}(k)$ is the estimated value of $\boldsymbol{\Phi}(k)$.

1.3.2 PPJM estimation algorithm

Considering the following estimation criteria function:

$$\begin{aligned} J(\boldsymbol{\Phi}(k)) = {} & \| \Delta\boldsymbol{y}(k) - \phi_1(k)\Delta\boldsymbol{y}(k-1) \\ & - \phi_2(k)\Delta\boldsymbol{u}(k-1) \|^2 \\ & + \mu \| \boldsymbol{\Phi}(k) - \hat{\boldsymbol{\Phi}}(k-1) \|^2 \end{aligned} \quad (10)$$

Deriving and making it equal to zero, the following expression can be obtained:

$$\begin{aligned} \hat{\boldsymbol{\Phi}}(k) = {} & \hat{\boldsymbol{\Phi}}(k-1) \\ & + \eta\Delta\boldsymbol{H}(k-1)\frac{\boldsymbol{y}(k) - \boldsymbol{y}(k-1)}{\mu + \| \Delta\boldsymbol{H}(k-1) \|^2} \\ & - \eta\Delta\boldsymbol{H}(k-1)\frac{\hat{\boldsymbol{\Phi}}^T(k-1)\Delta\boldsymbol{H}(k-1)}{\mu + \| \Delta\boldsymbol{H}(k-1) \|^2} \end{aligned} \quad (11)$$

where $\Delta\boldsymbol{H}(k-1) = [\Delta\boldsymbol{y}(k-1), \Delta\boldsymbol{u}(k-1)]^{\mathrm{T}}$, when $\| \hat{\boldsymbol{\Phi}}(k) \| \leqslant \varepsilon$ or $\| \Delta\boldsymbol{H}_{L_y, L_u}(k-1) \| \leqslant \varepsilon$ or $sign(\hat{\varphi}_2(k)) \neq sign(\hat{\varphi}_2(1))$, $\hat{\boldsymbol{\Phi}}(k) = \hat{\boldsymbol{\Phi}}(1)$.

1.4 Stability analysis

Theorem 1 Eq. (5) represents the discrete dynamics model of a space manipulator, $\boldsymbol{y}(k+1)$ is partial differential continuous with respect to the control outputs $\boldsymbol{y}(k)$ and control inputs $\boldsymbol{u}(k)$, therefore the system is generalized Lipschitz. For $\boldsymbol{y}^*(k+1) =$

$\boldsymbol{y}^*(k) = const$, there is a positive number $\lambda_{\min}$, when $\lambda > \lambda_{\min}$, gives:

1) The tracking error of the system is asymptotically convergent.

2) The closed-loop system is BIBO, for which the input and the output are bounded.

Proof The proof process involves 2 steps. The first step proves the boundedness of the PPJM estimation value and the second step proves the convergence of the tracking error and the BIBO stability of the system.

Step 1 $\tilde{\phi}(k) = [\hat{\phi}_1(k) - \phi_1(k); \hat{\phi}_2(k) - \phi_2(k)]$ denotes the estimation error. Since the system satisfies the Lipschitz condition, therefore, $\| \phi_1 \|$ and $\| \phi_2 \|$ are bounded, then $\| \phi_1 \| \leqslant a_1$, $\| \phi_2 \| \leqslant a_2$.

Subtract $\phi_1(k)$ and $\phi_2(k)$ respectively from the Eq. (11), as follows:

$$\tilde{\phi}_1(k) = \tilde{\phi}_1(k-1)\left[I - \frac{\eta \Delta y(k-1)\Delta y(k-1)^{\mathrm{T}}}{\mu + \| \Delta y(k-1) \|^2 + \| \Delta u(k-1) \|^2}\right] - \tilde{\phi}_2(k-1)\frac{\eta \Delta u(k-1)\Delta y(k-1)^{\mathrm{T}}}{\mu + \| \Delta y(k-1) \|^2 + \| \Delta u(k-1) \|^2} + \phi_1(k-1) - \phi_1(k) \tag{12}$$

$$\tilde{\phi}_2(k) = \tilde{\phi}_2(k-1)\left[I - \frac{\eta \Delta u(k-1)\Delta u(k-1)^{\mathrm{T}}}{\mu + \| \Delta y(k-1) \|^2 + \| \Delta u(k-1) \|^2}\right] - \tilde{\phi}_1(k-1)\frac{\eta \Delta y(k-1)\Delta u(k-1)^{\mathrm{T}}}{\mu + \| \Delta y(k-1) \|^2 + \| \Delta u(k-1) \|^2} + \phi_2(k-1) - \phi_2(k) \tag{13}$$

Since $\| \phi_1(k-1) - \phi_1(k) \| \leqslant 2a_1$, $\| \phi_2(k-1) - \phi_2(k) \| \leqslant 2a_2$, take the norm of the above 2 formulas, the following expression can be obtained:

$$\| \tilde{\phi}_1(k) \| \leqslant \| \tilde{\phi}_1(k-1) \| \times \left\| I - \frac{\eta \| \Delta y(k-1) \|^2}{\mu + \| \Delta y(k-1) \|^2 + \| \Delta u(k-1) \|^2} \right\| \| \tilde{\phi}_2(k-1) \| \times \left\| \frac{\eta \| \Delta u(k-1) \| \, \| \Delta y(k-1)^{\mathrm{T}} \|}{\mu + \| \Delta y(k-1) \|^2 + \| \Delta u(k-1) \|^2} \right\| 2a_1 \tag{14}$$

$$\| \tilde{\phi}_2(k) \| \leqslant \| \tilde{\phi}_2(k-1) \| \times \left\| I - \frac{\eta \| \Delta u(k-1) \|^2}{\mu + \| \Delta y(k-1) \|^2 + \| \Delta u(k-1) \|^2} \right\| \| \tilde{\phi}_1(k-1) \| \times \left\| \frac{\eta \| \Delta y(k-1) \| \, \| \Delta u(k-1)^{\mathrm{T}} \|}{\mu + \| \Delta y(k-1) \|^2 + \| \Delta u(k-1) \|^2} \right\| 2a_2 \tag{15}$$

Since $\mu > 0$, $\eta \in (0, 2]$, the following can be obtained

$$\left\| I - \frac{\eta \| \Delta y(k-1) \|^2}{\mu + \| \Delta y(k-1) \|^2 + \| \Delta u(k-1) \|^2} \right\| \in (0,1) \tag{16}$$

$$\left\| \frac{\eta \| \Delta u(k-1) \| \, \| \Delta y(k-1)^{\mathrm{T}} \|}{\mu + \| \Delta y(k-1) \|^2 + \| \Delta u(k-1) \|^2} \right\| \in (0,1) \tag{17}$$

$$\left\| I - \frac{\eta \| \Delta u(k-1) \|^2}{\mu + \| \Delta y(k-1) \|^2 + \| \Delta u(k-1) \|^2} \right\| \in (0,1) \tag{18}$$

$$\left\| \frac{\eta \| \Delta y(k-1) \| \, \| \Delta u(k-1)^{\mathrm{T}} \|}{\mu + \| \Delta y(k-1) \|^2 + \| \Delta u(k-1) \|^2} \right\| \in (0,1) \tag{19}$$

Therefore, there are constants b_1, b_2, b_3, $b_4 \in (0, 1)$, which make the following formula true:

$$\begin{bmatrix} \left\| \tilde{\phi}_1(k) \right\| \\ \left\| \tilde{\phi}_2(k) \right\| \end{bmatrix} \leqslant \begin{bmatrix} b_1 & b_2 \\ b_3 & b_4 \end{bmatrix} \begin{bmatrix} \left\| \tilde{\phi}_1(k-1) \right\| \\ \left\| \tilde{\phi}_2(k-1) \right\| \end{bmatrix} + \begin{bmatrix} 2a_1 \\ 2a_2 \end{bmatrix} \tag{20}$$

Thus, the boundedness of the $\phi(k)$ and $\tilde{\phi}(k)$ can be proved.

Step 2 Defining

$$\boldsymbol{s}(k) = \boldsymbol{e}(k) = \boldsymbol{y}^*(k) - \boldsymbol{y}(k) \tag{21}$$

According to Eq. (6), the following expression can be obtained:

$$\begin{aligned} \boldsymbol{s}(k+1) &= \boldsymbol{e}(k+1) \\ &= \boldsymbol{y}^*(k) - \boldsymbol{y}(k) - (\boldsymbol{y}(k+1) - \boldsymbol{y}(k)) \\ &= \boldsymbol{s}(k) - (\phi_1(k)\Delta \boldsymbol{y}(k) + \phi_2(k)\Delta \boldsymbol{u}(k)) \end{aligned} \tag{22}$$

Because of the boundedness of $\phi(k)$ and according to Lyapunov's theorem, the system motion trajectory tends to a balance state $\boldsymbol{s}(k)$, so the tracking error of the system is convergent, which means $\lim_{k\to\infty} e(k) = 0$. The conclusion (1) is proved.

It can be proved that the error between the actual output value and the expected value eventually reaches zero. Substituting Eqs(6) and (12) into Eq. (19)

$$\begin{aligned} \boldsymbol{e}(k+1) &= \boldsymbol{e}(k) - \phi_1(k)\Delta \boldsymbol{y}(k) - \phi_2(k)\Delta \boldsymbol{u}(k) \\ &= \boldsymbol{e}(k) - \boldsymbol{\Phi}^{\mathrm{T}}(k)\Delta \boldsymbol{H}(k) \end{aligned} \tag{23}$$

Since $\lim_{k\to\infty} e(k) = 0$ and $\boldsymbol{\Phi}(K)$ are bounded in the above equation, it can be obtained that $\lim_{k\to\infty} \Delta \boldsymbol{H}(k) = 0$, which means $\boldsymbol{y}(k)$ and $\boldsymbol{u}(k)$ are bounded. The conclusion (2) is obtained.

It can be proved that the MFAC control algorithm provides a bounded input for the 2 degrees of freedom of space manipulator control system so that the tracking error of the system converges, which can ensure the stability of the system.

2 Simulation test

2.1 Simulation parameters

To consummate the simulation structure and in-

spired by the modeling of the space manipulator by Gao[16], the structure of the 2 degrees of freedom space manipulator in the gravity environment is defined as Fig. 2.

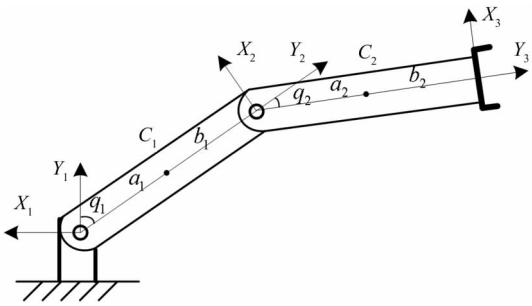

Fig. 2 The structure of two degrees of freedom space manipulator in gravity environment

The kinematics parameters in the ground gravity environment are indicated in Table 1.

Table 1 The kinematics parameters of the space manipulator in the ground environment

Link	m_i (kg)	I_i (kg · m^2)	a_i (m)	I_i (m)
1	4	0.333	0.5	1
2	3	0.250	0.5	1

When the space manipulator operates in a microgravity environment, the pedestal posture is out of control because of the gravity release. Thus, the pedestal of the space manipulator can be assumed to be a pseudo-mechanical space manipulator which consists of two moving joints and one rotating joint that rotates around its center of mass. The structure schematic is shown in Fig. 3.

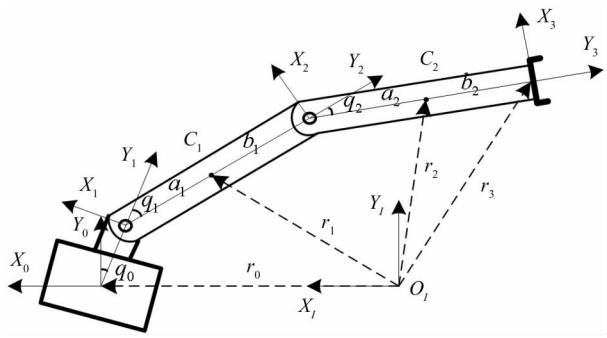

Fig. 3 The structure of two degrees of freedom space manipulator in microgravity environment

The kinematics parameters in the space microgravity environment are indicated in Table 2.

Table 2 The kinematics parameters of the space manipulator in the space environment

Link	m_i (kg)	I_i (kg · m^2)	a_i (m)	b_i (m)
0	40	6.667	–	0.5
1	4	0.333	0.5	0.5
2	3	0.250	0.5	0.5

The initial position of the end of the space manipulator is set as (1.15, 0.14), and the desired trajectory of the end of the space manipulator is inspired by Gao[16], which is set as

$$\begin{cases} x_d = 0.28\cos(\dfrac{\pi t}{5}) + 0.85 \\ y_d = 0.28\cos(\dfrac{\pi t}{5}) \end{cases} \tag{24}$$

Based on the desired trajectory, the angle of the joint can be obtained by inverse kinematics solution. The control system is established under the environment of Matlab R2016b. To verify the superiority of the MFAC controller, the simulation results are compared with the ones that are obtained according to traditional PD control strategy. For the comparison purpose, the simulation experiment in this paper does not change the controller parameters at different operation condition, which are the same as the ground debugging. Meanwhile, both strategies should follow the same initial conditions.

The PD controller parameters are set as follows:

$$\boldsymbol{\tau} = \boldsymbol{K}_P + \boldsymbol{K}_d\dot{e} \tag{25}$$

where $\boldsymbol{K}_P = diag(250, 250)$ $\boldsymbol{K}_d = diag(50, 50)$.

2.2 Simulation result

The simulation time is 10 s, the simulation results are shown as follows.

Fig. 4 and Fig. 5 show the joint angle tracking and end-effector tracking results in different gravity environment, respectively. It can be directly observed from Fig. 4 that PD control can follow the desired trajectory more precisely, while there is a little deviation for MFAC strategy. However, Fig. 5 shows that MFAC can follow the desired trajectory with a high accuracy in microgravity environment, while PD control completely deviates from the desired trajectory. Fig. 6 shows the tracking error of end-effector of the space manipulator in different environment. The error of PD control is nearly 0 in gravity environment. When gravity condition changes, its error peak is almost over 0.2 m in microgravity environment. Meanwhile, the error of MFAC strategy remains at a low level in different gravity environment, and the maximum error of 0.025 m for gravity environment as well as the maximum error of nearly 0 for microgravity environment.

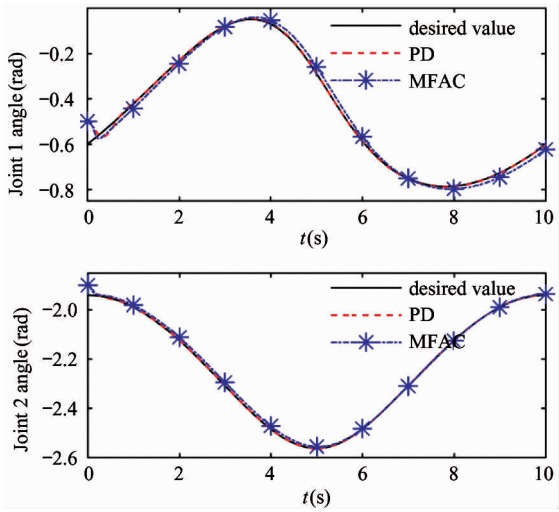

(a) Joint angle tracking in gravity environment

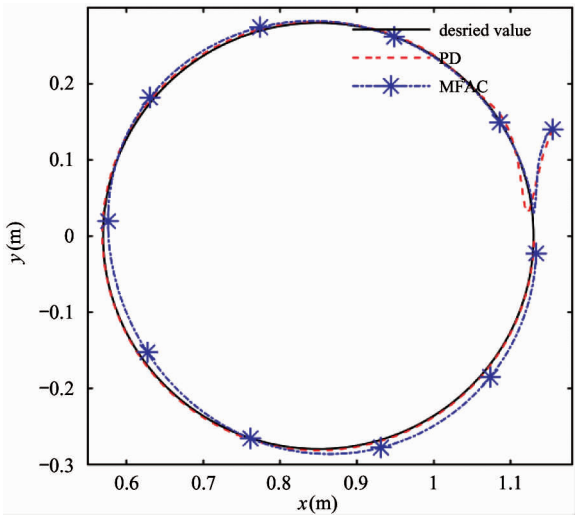

(b) End-effector tracking in gravity environment

Fig. 4 Simulation results without disturbance in gravity environment

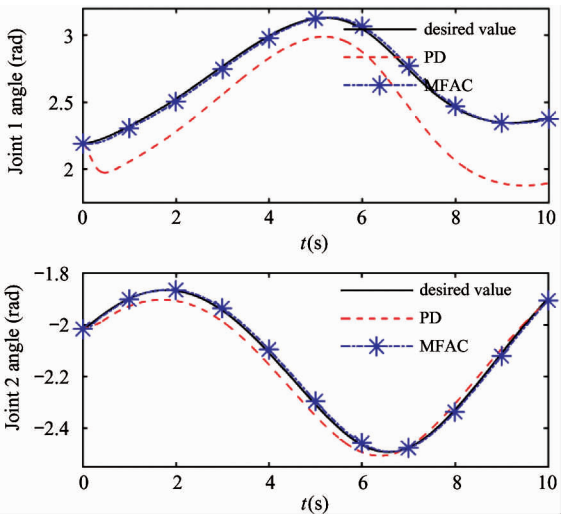

(a) Joint angle tracking in microgravity environment

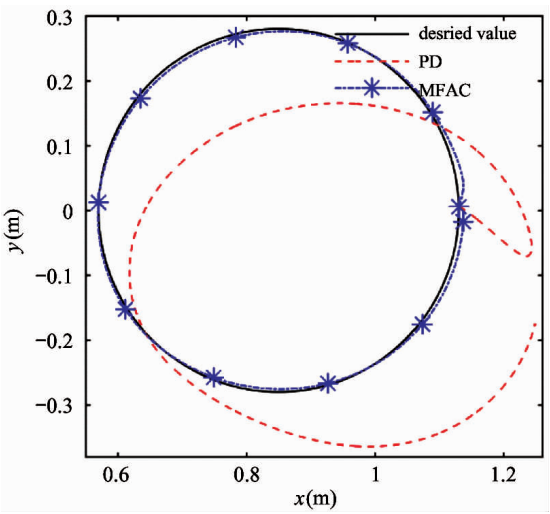

(b) End-effector tracking in microgravity environment

Fig. 5 Simulation results without disturbance in microgravity environment

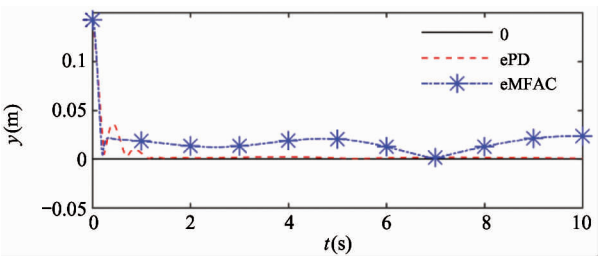

(a) End-effector tracking error in gravity environment

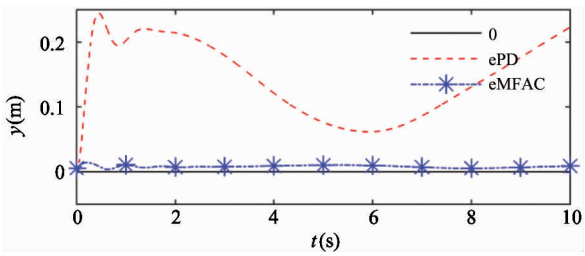

(b) End-effector tracking error in microgravity environment

Fig. 6 Tracking error of different environment

Since the space environment has many uncertain disturbances, it is considered to add a disturbance signal to inspect the anti-disturbance performance of both control strategies . Fig. 7 shows the disturbance signal which is added to the control system. The amplitude of the signal is 5 which is added in the 5th second of the simulation and removed at the 7th second.

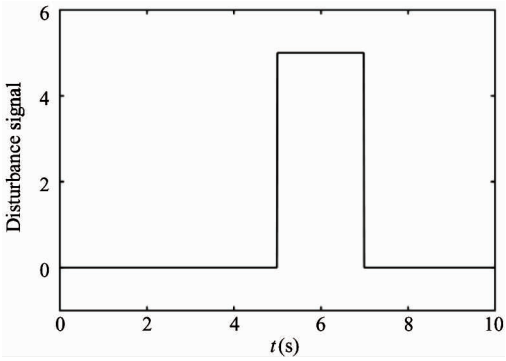

Fig. 7 Disturbance signal

Fig. 8 and Fig. 9 present the tracking of end-effector when the external disturbance signal is considered. It can be obtained from Fig. 8 that MFAC strategy can follow the desired trajectory more quickly after the disturbance signal occurs. Moreover, the fluctuation value of MFAC strategy is smaller than the one of PD control strategy in both environments. Fig. 10 shows the tracking error of the end track does not change much when it is compared to the one in Fig. 6 except that the error of both control strategies becomes larger after adding the disturbance signal.

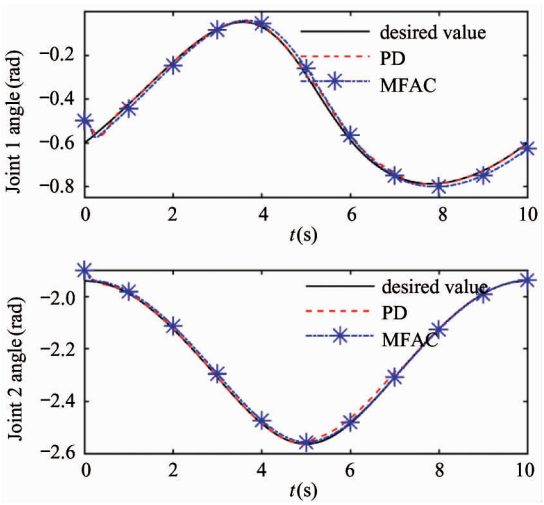

(a) Joint angle tracking in gravity environment

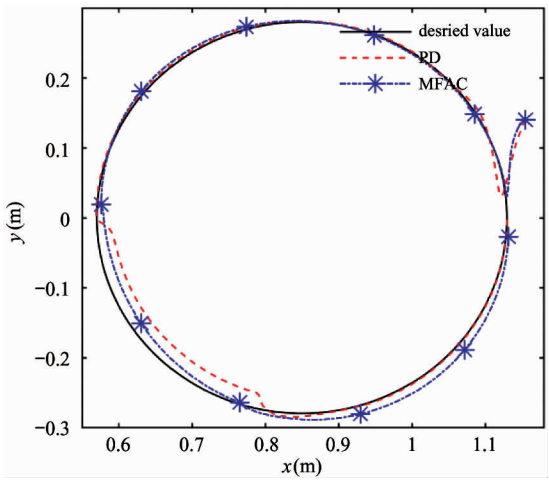

(b) End-effector tracking in gravity environment

Fig. 8 Simulation results with disturbance at gravity environment

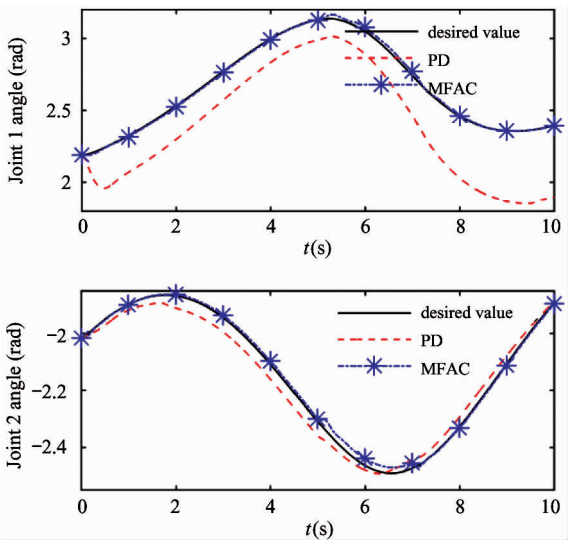

(a) Joint angle tracking in microgravity environment

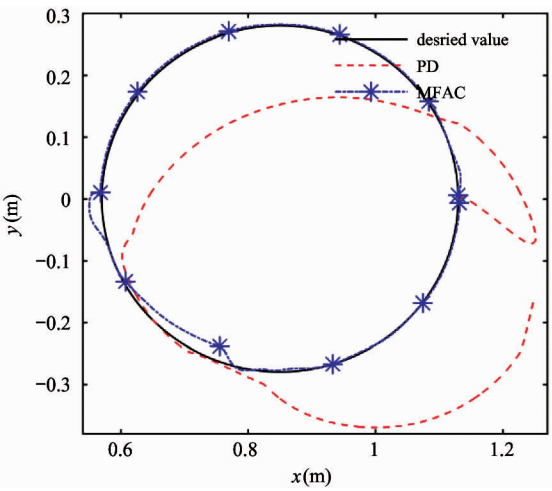

(b) End-effector tracking in microgravity environment

Fig. 9 Simulation results with disturbance at microgravity environment

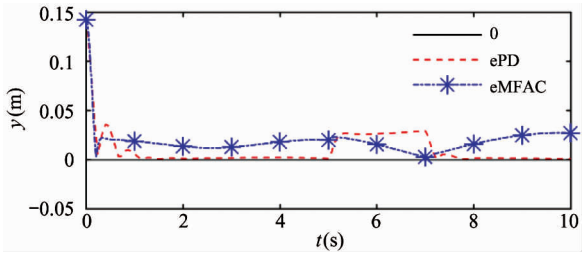

(a) Ground environment end tracking error

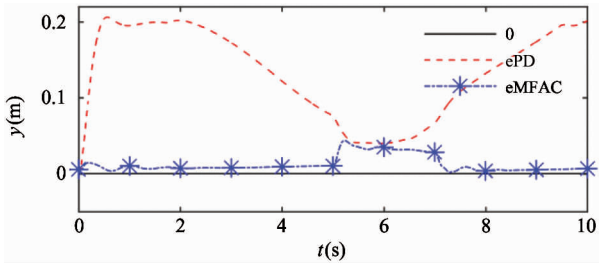

(b) Space environment end tracking error

Fig. 10 Simulation results with external disturbance

3 Conclusions

The trajectory tracking problem of the space manipulator is investigated, aiming at the inaccuracy of the tracking control of the end of the manipulator caused by the change of gravity, the dynamic linearization of the dynamic equation is obtained, and the input and output relationship of the system is obtained. Based on this relationship, MFAC controller is designed to solve the inaccuracy trajectory tracking control of the space manipulator under different gravity environment. Finally, simulation results are given to show the effectiveness of the proposed approach.

In the future, we will continue to improve the control accuracy of the system, and also consider the flexibility and clearance of the space manipulator mechanism. Moreover, how to extend the anti-interference ability of the control system is also the future work.

References

[1] Shan M, Guo J, Gill E. Review and comparison of active space debris capturing and removal methods[J]. *Progress in Aerospace Science*, 2016, 80: 18-32

[2] Flores-Abad A, Ma O, Pham K, et al. A review of space robotics technologies for on-orbit servicing[J]. *Progress in Aerospace Sciences*, 2014, 68: 1-26

[3] Rybus T. Obstacle avoidance in space robotics: review of major challenges and proposed solutions[J]. *Progress in Aerospace Sciences*, 2018, 101: 31-48

[4] Edeson R, Aglietti G S, Tatnall A R L. Conventional stable structures for space optics: the state of the art[J]. *Acta Astronautics*, 2010, 66: 13-32

[5] Kazuya Y. Space manipulator dynamics and control: to orbit, from orbit, and future[J]. *Robotics Research*, 1993, DOI: 10.1007/978-1-447/-0765-1_54

[6] Walker M W, Wee L B. Adaptive control of space-based robot manipulators[J]. *IEEE Transactions on Robotics and Automation*, 1991, 7(6): 828-835

[7] Kim Y H, Lewis F L. Neural network output feedback control of robot manipulators[J]. *IEEE Transactions on Robotics and Automation*, 1999, 15(2): 301-309

[8] Qin L, Liu F C, Liang L H. Fuzzy adaptive robust control for space robot considering the effect of the gravity[J]. *Chinese Journal of Aeronautics*, 2014, 27(6): 1562-1570

[9] Qin L, Liu F C, Liang L H. The application of adaptive backstepping sliding mode for hybrid humanoid robot arm trajectory tracking control[C]//International Conference on Advanced Mechatronic Systems, Luoyang, China, 2013: 730-735

[10] Gao B B, Cao R M, Hou Z S, et al. Model-free adaptive MIMO control algorithm application in polishing robot [C]//IEEE 6th Data Driven Control and Learning Systems Conference, Chongqing, China, 2017: 135-140

[11] Wang X F, Li X, Wang J H, et al. Data-driven model-free adaptive sliding mode control for the multi degree-of-freedom robotic exoskeleton[J]. *Information Sciences*, 2016, 327: 246-257

[12] Hou Z S. The Parameter Identification, Adaptive Control and Model Free Learning Adaptive Control for Nonlinear System[D]. Shenyang: Department of Automatic Control, Northeastern University, 1994 (In Chinese)

[13] Hou Z S, Jin S T. A novel data-driven control approach for a class of discrete-time nonlinear systems[J]. *IEEE Transactions on Control Systems Technology*, 2011, 19(6): 3107-3110

[14] Hou Z S, Jin S T. Data-driven model-free adaptive control for a class of MIMO nonlinear discrete-time systems [J]. *IEEE Transactions on Neural Networks*, 2011, 22(12): 2173-2188

[15] Hou Z S, Jin S T. Model-free Adaptive Control: Theory and Applications[M]. Beijing: Science Press, 2013: 91-122 (In Chinese)

[16] Gao J J. The Control Technology Research of a Typical Space Operation Mechanism During Both Ground Simulation and Space Application[D]. Qinhuangdao: Deparment of Automation, Yanshan University, 2013 (In Chinese)

Wen Yintang, born in 1978. He received his Ph. D degree in control science and engineering, Master's degree in precision instrumentation and mechanics, Bachelor's degree in automation at Yanshan University in 1999, 2007 and 2018 respectively. His current research interests include automation system integration and intelligent control.